

Supporting Information

© Copyright Wiley-VCH Verlag GmbH & Co. KGaA, 69451 Weinheim, 2020

¹¹C Radiolabeling of anle253b: a Putative PET Tracer for Parkinson's Disease That Binds to α -Synuclein Fibrils in vitro and Crosses the Blood-Brain Barrier

Andreas Maurer,* Andrei Leonov, Sergey Ryazanov, Kristina Herfert, Laura Kuebler, Sabrina Buss, Felix Schmidt, Daniel Weckbecker, Ruth Linder, Dirk Bender, Armin Giese, Bernd J. Pichler, and Christian Griesinger*© 2020 The Authors. Published by Wiley-VCH Verlag GmbH & Co. KGaA. This is an open access article under the terms of the Creative Commons Attribution Non-Commercial NoDerivs License, which permits use and distribution in any medium, provided the original work is properly cited, the use is non-commercial and no modifications or adaptations are made.

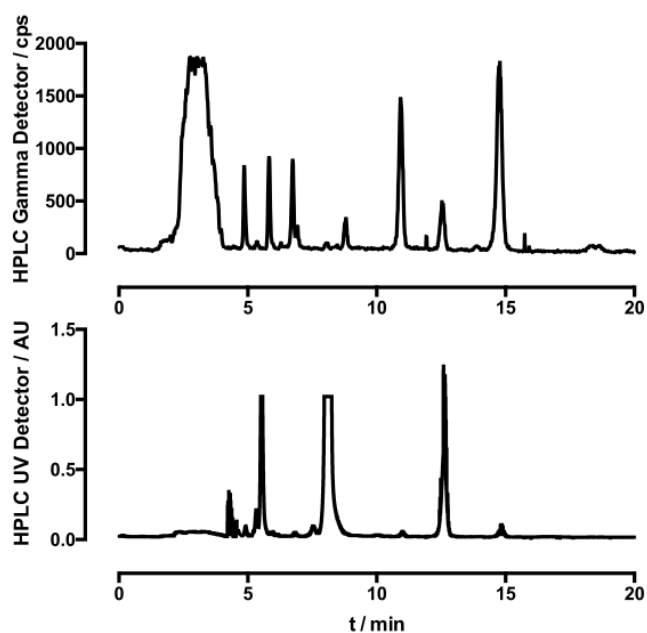
Table of Contents

Supplemental Results	1
Radiomethylation with bicarbonate.....	1
Serum stability.....	2
Molar activity experiments.....	2
Material and Methods:.....	3
Synthesis of ruli22 (3)	4
Synthesis of anle253b (2)	5
Synthesis of 4 and 5	6
Non-radioactive methylation reactions	8
Synthesis of quinuclidine- <i>N</i> -oxide (QNO).....	8
Production of [¹¹ C]methyl iodide and [¹¹ C]methyl triflate.....	10
Substitutive radiomethylation of 3	10
Reductive radiomethylation of 3	11
Formulation of [¹¹ C] 2	11
[¹¹ C] 2 quality control and calculation of specific activity.....	11
Serum stability analysis	11
Production of αSyn fibrils.....	11
Fibril characterization	12
αSyn fibril binding assay for ¹¹ C	12
Tritium binding assay	13
Dynamic biodistribution analysis	13
Supplemental References.....	15

Supplemental Results

Radiomethylation with bicarbonate

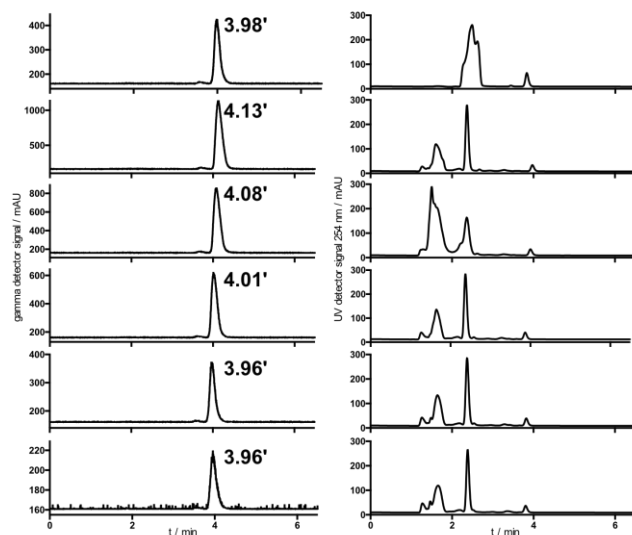
Substitutive radiomethylation using sodium bicarbonate partially suppresses the formation of **4** and **5** in favor of **2** but only yields low radiochemical conversion (Supplemental Figure 1).



Supplemental Figure 1: Radiomethylation of 1 mg **3** in 300 μ L DMSO containing 0.5 mg sodium bicarbonate using [^{11}C]MeI. A small amount of non-radioactive **2** was added to aid identification of the product (12' retention time). Radioactive **2** was formed but most radioactivity was found in the injection peak at \sim 3 min.

Serum stability

The tracer was incubated with rat serum at 37 $^{\circ}\text{C}$, and samples were analyzed by HPLC as described in Materials and Methods (Supplemental Figure 2).

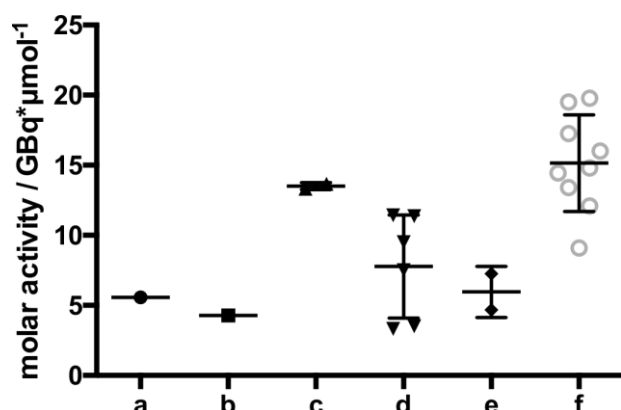


Supplemental Figure 2: Serum stability analysis of [^{11}C]**2**. Left column shows radioactivity traces with retention time of the peaks, right column the respective UV absorption at 254 nm. The tracer was incubated before (first row) and after addition of rat serum and incubation at 37 $^{\circ}\text{C}$ for 0, 15, 30, 60 and 90 min (from second row to bottom). No signs of metabolic degradation were observed. The shift in retention times can be attributed to successive loading of the column with serum components. The UV signal differs at the first and the third timepoint, presumably indicating varying precipitation of serum components.

Molar activity experiments

Molar radioactivity was dependent on the oxidizing agent (TMAO or quinuclidin-*N*-oxide, QNO), solvent (dimethyl formamide, diethyl formamide, dimethyl acetamide,

acetonitrile) and beam time (11.7 μAh , 37 μAh), but could not be improved to values above 20 GBq/ μmol . (Supplemental Figure 3).



Supplemental Figure 3: Molar activity of $[^{11}\text{C}]\mathbf{2}$ at EOS is similarly low under different conditions: DMF, TMAO, 11.7 μAh (a), DMA, TMAO, 11.7 μAh (b), MeCN, TMAO, 11.7 μAh (c), DEF, TMAO, 11.7 μAh (d), DEF, QNO, 11.7 μAh (e), DEF, TMAO, 35 μAh (f). Single syntheses are plotted, mean value and standard deviation are indicated.

Material and Methods:

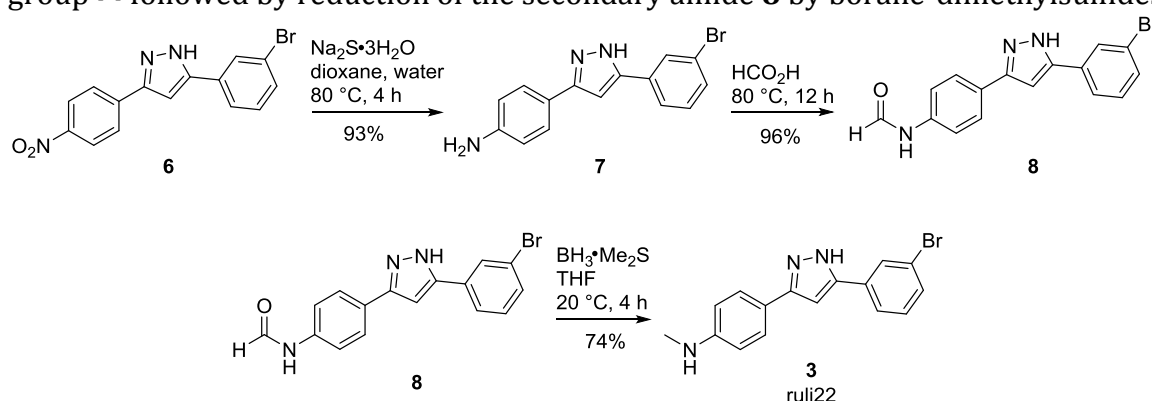
All solvents and reagents were obtained from commercial suppliers in at least analytical quality. Solvents and reagents were purified as described by Armarego et al.^[1] when necessary. Target gas was purified using a high-pressure gas dryer (Alltech), helium and hydrogen gas supply for radiosynthesis modules was of 5.0 and 6.0 purity, respectively. NMR spectra were recorded at a temperature of 298 K on a 400 MHz Bruker Avance spectrometer (Bruker AG, Rheinstetten, Germany) equipped with TXI HCN z-grad probe. Spectra were processed with XWINNMR 3.1 (Bruker AG, Karlsruhe, Germany). ^1H NMR chemical shifts (δ) are reported in parts per million (ppm) relative to tetramethylsilane (TMS) (δ 0.00 in CDCl_3), $[\text{D}_5]\text{DMSO}$ (δ 2.5 in $[\text{D}_6]\text{DMSO}$), or 4,4-dimethyl-4-silapentane-1-sulfonic acid sodium salt (DSS) (δ 0.00 in D_2O) as internal standards. Data are reported as follows: chemical shift, integration, multiplicity (s = singlet, d = doublet, t = triplet, b = broadened, m = multiplet), coupling constants (J, given in Hz). ^{13}C NMR chemical shifts (δ) are reported in parts per million (ppm) relative to CDCl_3 (δ 77.0), $[\text{D}_6]\text{DMSO}$ (δ 39.7), or DSS (δ 0.00 in D_2O) as internal standards. The following experiments were used to record the resonances of the compounds: ^1H -1D, ^{13}C -1D NMR spectra and ^{13}C -APT (attached proton test with a single J-evolution time of 1/145 s, spectra are processed such that quaternary and methylene groups have positive sign and methyl and methine groups negative sign). To resolve overlap of resonances and recover undetectable resonances in ^1H and APT spectra, 2D- $^{13}\text{C},^1\text{H}$] HSQC (heteronuclear single quantum coherence), 2D- $^{13}\text{C},^1\text{H}$] HMBC (heteronuclear multiple bond correlation) and 2D-NOESY were recorded for some compounds. 1,3-diarylpropane-1,3-diones are presented in the figures as diketones despite the fact that the enol form dominates the spectra. Melting points were determined with a Stuart Scientific (BIBBY, UK) capillary apparatus and are uncorrected. Thin layer chromatography (TLC) was performed on Macherey-Nagel precoated sheets, 0.25 mm Polygram SIL G/UV₂₅₄ plates, and compounds were detected with UV and/or by charring with 10 % (w/w) ethanolic phosphomolybdic acid reagent followed by heating at 200 $^\circ\text{C}$. Flash column chromatography was performed on Merck silica gel 60 (0.015-0.040 mm). Analytical and preparative high performance liquid chromatography (HPLC) was performed using a Waters HPLC system with a Waters 996 Photodiode Array Detector.

All separations involved a mobile phase of 0.1% trifluoroacetic acid (TFA) (v/v) in water (solvent A) and 0.1% TFA in acetonitrile (solvent B). HPLC was performed using reversed-phase (RP) column Eurospher RP 18, 100 Å, 5µm, 250×4.6 mm (analytical) and 250×16 mm (preparative) at flow rates of 1 mL×min⁻¹ (analytical) and 7 mL×min⁻¹ (preparative). Electrospray ionization mass spectrometry (ESI MS) and LC MS analyses were obtained on a Waters Micromass ZQ 4000 mass spectrometer in conjunction with the Waters HPLC apparatus described above. High-resolution mass spectra (HRMS) were recorded on MS Finnigan LCQ (Ion-Trap) mass spectrometer and are reported in m/z. The calculated logP values of the listed compounds were determined using two different programs, ACD/ChemSketch, Product Version 12.01 (logP ac), and Molinspiration Cheminformatics (logP mi).

Radiochemistry modules Tracerlab FX MeI and M (GE Healthcare) were used in their original configuration according to the manufacturer's recommendations. Female Sprague Dawley rats were obtained from Charles River (Sulzfeld, Germany) at an age of 10 weeks and kept in individually-vented cages under standardized environmental conditions. Food and water were provided *ad libitum*. All experiments involving animals were conducted in accordance with the German animal protection laws after approval by the local authorities (Regierungspräsidium Tübingen).

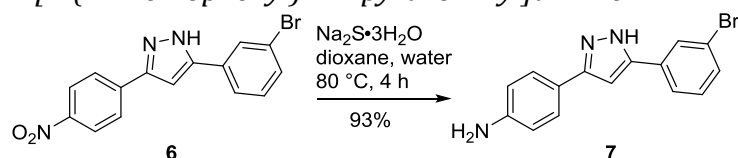
Synthesis of ruli22 (**3**)

The title compound was synthesized [2] as shown in Supplemental Scheme 1 starting from 5-(3-bromophenyl)-3-(4-nitrophenyl)-1H-pyrazole **6** [3] in three steps including a selective reduction of the nitro group,[4] formylation of the resulting aromatic amino group [5] followed by reduction of the secondary amide **8** by borane-dimethylsulfide.[6]



Supplemental Scheme 1: Synthesis of **3**.

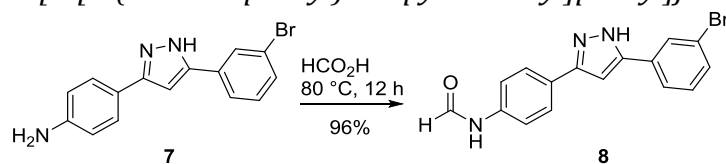
4-[5-(3-Bromophenyl)-1H-pyrazol-3-yl]aniline **7**.



To a suspension of 5-(3-bromophenyl)-3-(4-nitrophenyl)-1H-pyrazole (**6**) (5.6 g, 16.3 mmol) in dioxane (60 mL) a warm (ca. 60 °C) solution of sodium sulfide trihydrate (5.4 g, 40.7 mmol) in water (45 mL) was added in one portion at 80 °C. The mixture was stirred for 4 h, cooled down to RT and poured into ice water (200 mL). After 1 h stirring at 0 °C the resulting precipitate was filtered off, washed with cold water (2×50 mL) and air dried. The crude product (4.95 g) was dissolved in MeOH, filtered and evaporated to afford 4-[5-(3-bromophenyl)-1H-pyrazol-3-yl]aniline (4.78 g, 15.2 mmol, 93%) as

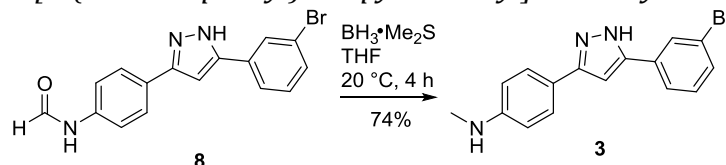
orange solid. **¹H NMR** (400 MHz, DMSO-*d*₆), **¹³C-NMR** (75 MHz, DMSO-*d*₆), and **ESI-MS** spectra were identical to previous literature reports.^[3] **m.p.**: 201 °C.

N-[4-[5-(3-Bromophenyl)-1*H*-pyrazol-3-yl]phenyl]formamide **8**.



A solution of 4-[5-(3-bromophenyl)-1*H*-pyrazol-3-yl]aniline (**7**) (4 g, 12.7 mmol) in formic acid (20 mL) was stirred at 80 °C for 12 h. After cooling to room temperature (RT) the mixture was poured into ice water (200 mL), the resulting precipitate was filtered off, washed with water and air dried at 50 °C for 24 h to afford *N*-[4-[5-(3-bromophenyl)-1*H*-pyrazol-3-yl]phenyl]formamide (4.16 g, 12.2 mmol, 96%) as a tan solid. **¹H NMR** (400 MHz, DMSO-*d*₆+1% v/v DCl): δ = 10.42 (s, 0.3 H), 10.26 (d, *J* = 1.1 Hz, 0.1 H), 8.87 (t, *J* = 4.8 Hz, 0.2 H), 8.30 (s, 0.6 H), 8.05 (s, 1 H), 7.85 (d, *J* = 7.8 Hz, 1 H), 7.79 (d, *J* = 8.6 Hz, 2 H), 7.69 (d, *J* = 8.6 Hz, 1.5 H), 7.52 (m, 1 H), 7.41 (t, *J* = 7.8 Hz, 1 H), 7.30 (d, *J* = 8.5 Hz, 0.5 H), 7.24 (m, 1 H). **¹³C-NMR** (75 MHz, DMSO-*d*₆+ 1% v/v DCl): δ = 162.7, 162.6, 159.9, 159.8, 146.9, 146.4, 138.3, 138.2, 134.4, 131.2, 130.6, 127.8, 126.5, 126.1, 126.0, 124.3, 124.0, 122.5, 119.6, 119.5, 117.8, 117.7, 100.1. **ESI-MS**: *m/z* (MeCN, positive mode): calcd for C₁₆H₁₂⁷⁹BrN₃O [M+H]⁺: 342.03 found: 341.95. **m.p.**: 260 °C.

4-[5-(3-Bromophenyl)-1*H*-pyrazol-3-yl]-*N*-methylaniline (**3**, *ruli22*).



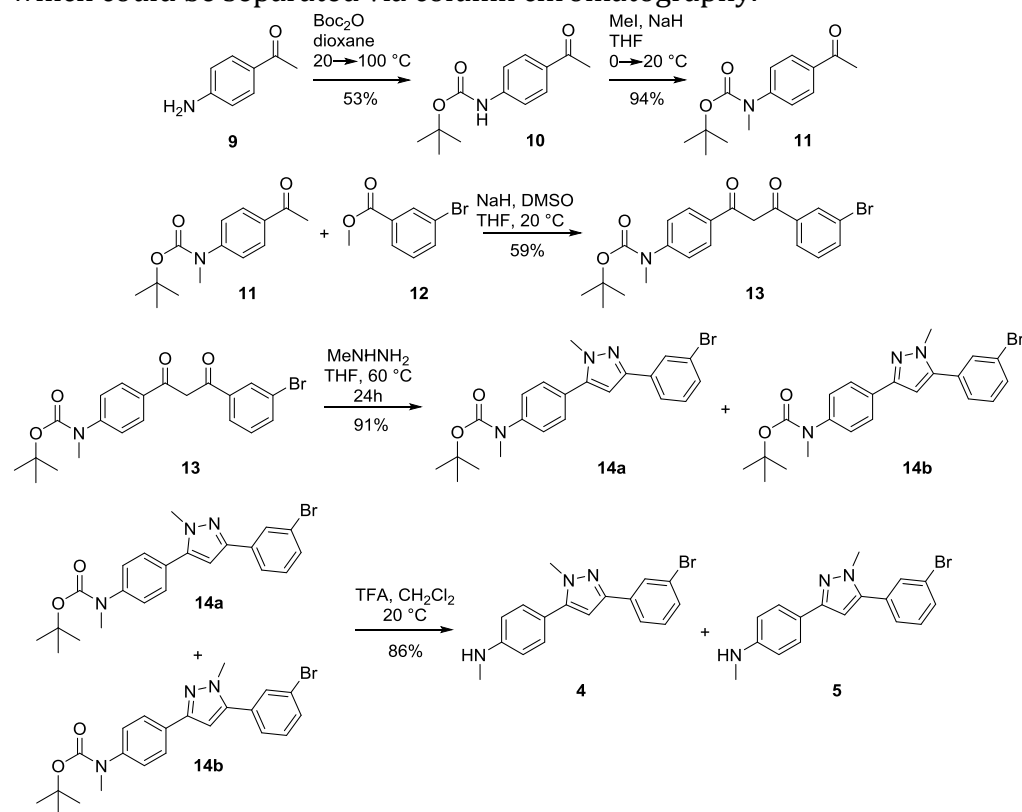
Borane dimethylsulfide (5.55 mL, 4.44 g, 58.4 mmol, 2.00 Eq.) was added dropwise over 10 min at 0 °C to a suspension of *N*-[4-[5-(3-Bromophenyl)-1*H*-pyrazol-3-yl]phenyl]formamide (**8**) (10.0 g, 29.2 mmol, 1.00 Eq.) in THF. The solution was stirred for 30 min at 0 °C and for 2 h at RT. An additional amount of borane dimethylsulfide (1 mL, 1.25 g, 16.5 mmol, 0.56 Eq.) and THF (15 mL) were added and stirred for 2 h at RT. After addition of MeOH (83 mL) and HCl (1 M, 250 mL) the solution was stirred overnight (15 h). A 10 % aq. NaOH solution (150 mL, pH = 13) was added and the mixture was stirred for 30 min. The mixture was extracted with EtOAc (150 mL), washed with aq. NaHCO₃ (150 mL) and brine (150 mL) and dried over Na₂SO₄. Recrystallization (EtOH / H₂O = 1 / 1, 400 mL) provided the title compound (7.05 g, 21.5 mmol, 74 %) as a white solid. **¹H NMR** (400 MHz, DMSO-*d*₆+1% v/v 37% DCl in D₂O): δ = 8.04 (t, *J* = 1.8 Hz, 1 H), 7.85 (dt, *J* = 7.7, 1.3 Hz, 1 H), 7.76 (bd, *J* = 8.5 Hz, 2 H), 7.52 (dq, *J* = 7.9, 1.0 Hz, 1 H), 7.40 (t, *J* = 7.8 Hz, 1 H), 7.18 (s, 1 H), 7.08 (bd, *J* = 7.9 Hz, 2 H), 2.82 (s, 3 H). **¹³C-NMR** (75 MHz, DMSO-*d*₆+1% v/v 37% DCl in D₂O): δ = 147.1, 146.7, 144.3, 134.7, 131.2, 130.5, 127.7, 126.6, 124.2, 122.4, 117.0, 99.6, 32.6. **ESI-MS**: *m/z* (MeCN, positive mode): calcd for C₁₆H₁₅⁸¹BrN₃ [M+H]⁺: 330.04 found: 330.37. **m.p.**: 217 °C.

Synthesis of anle253b (2)

2 was synthesized as previously described.^[3]

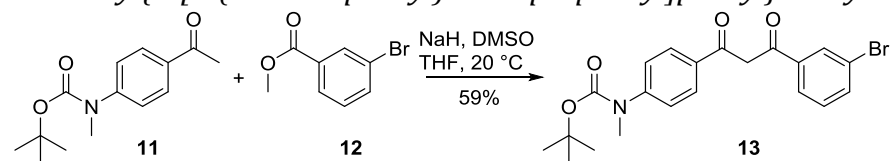
Synthesis of 4 and 5

The synthetic procedures of 4 and 5 are shown in Supplemental Scheme 2. The Claisen condensation of known acetophenone 11 [7] and methyl 3-bromobenzoate in the presence of sodium hydride gave diketone 13. The cyclisation reaction with methylhydrazine afforded protected pyrazoles 14a and 14b as an inseparable mixture of isomers. Final deprotection of Boc-protective group gave target products 4 and 5 which could be separated via column chromatography.



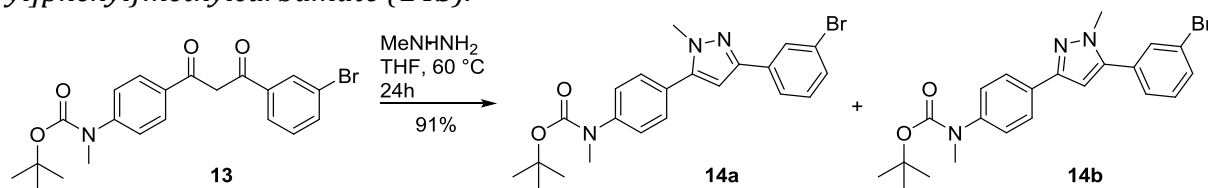
Supplemental Scheme 2: Synthesis of 4 and 5.

tert-Butyl{4-[3-(3-bromophenyl)-3-oxopropanoyl]phenyl}methylcarbamate 13.



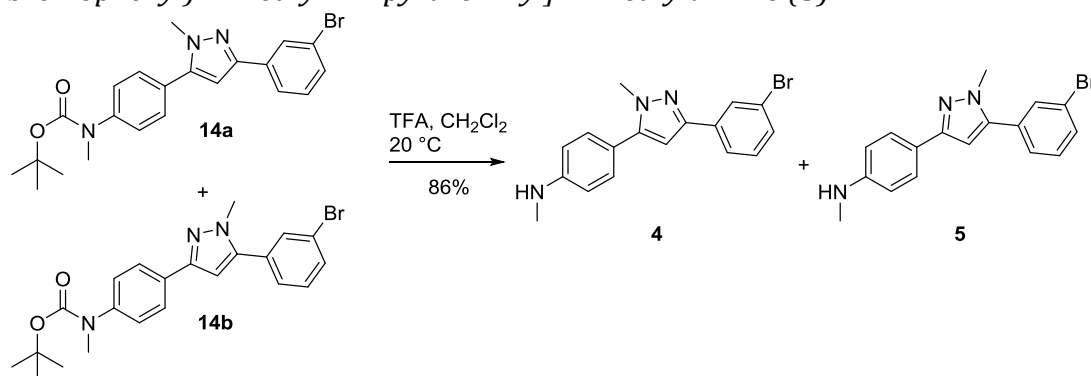
To a solution of *tert*-butyl *N*-(4-acetylphenyl)-*N*-methylcarbamate (2.49 g, 10 mmol) and methyl 3-bromobenzoate (2.58 g, 12 mmol) in DMSO (20 mL) and THF (5 mL) sodium hydride (60% in oil, 12 mmol, 480 mg) was added and stirred at 20 °C for 15 h. The reaction mixture was poured into a mixture of 125 mL ice water and 1 M sodium phosphate buffer pH 6 (25 mL), stirred for 30 min, and extracted with chloroform (3 × 40 mL). The solution was washed with brine, dried over Na₂SO₄ and concentrated in vacuo. The resulting oil was purified on 160 g silica gel (hexane:EtOAc = 3:1, R_f = 0.6) to afford the *tert*-butyl {4-[3-(3-bromophenyl)-3-oxopropanoyl]phenyl}methylcarbamate (2.54 g, 5.88 mmol, 59%) as a pale yellow crystalline solid. ¹H NMR (400 MHz, DMSO-d₆): δ = 8.34 (d, *J* = 1.7 Hz, 1 H), 8.18-8.12 (m, 3 H), 7.84 (m, 1 H), 7.55-7.46 (m, 3 H), 7.38 (s, 1 H), 3.27 (s, 3 H), 1.44 (s, 9 H). ¹³C-NMR (75 MHz, DMSO-d₆): δ = 185.8, 183.3, 153.7, 148.2, 137.3, 135.9, 131.5, 130.8, 130.3, 128.5, 126.8, 124.9, 122.8, 93.9, 80.9, 37.0, 28.3. **ESI-MS:** *m/z* (MeCN, positive mode): calcd for C₂₁H₂₃⁷⁹BrN₃O₄ [M+H]⁺: 432.08 found: 432.38. **m.p.:** 110 °C.

tert-Butyl {4-[3-(3-bromophenyl)-1-methyl-1*H*-pyrazol-5-yl]phenyl}methylcarbamate (**14a**) and *tert*-butyl {4-[5-(3-bromophenyl)-1-methyl-1*H*-pyrazol-3-yl]phenyl}methylcarbamate (**14b**).



To a solution of the *tert*-butyl {4-[3-(3-bromophenyl)-3-oxopropanoyl]phenyl}methylcarbamate **13** (432 mg, 1 mmol) in THF (8 mL) was added methylhydrazine (105 μ L, 92 mg, 2 mmol). After being stirred at 60 $^{\circ}$ C for 15 h additional methylhydrazine (53 μ L, 46 mg, 1 mmol) was added. The reaction mixture was stirred further for 6 h, cooled to RT, concentrated in vacuo and evaporated twice with methanol (10 mL). The residue was purified on 60 g silica gel (hexane:EtOAc = 3:1, R_f = 0.31-0.28) to afford the product as a mixture of isomers (403 mg, 0.91 mmol, 91%) as a yellowish glass. The mixture was used for the next step.

4-[3-(3-Bromophenyl)-1-methyl-1*H*-pyrazol-5-yl]-*N*-methylaniline (**4**) and 4-[5-(3-bromophenyl)-1-methyl-1*H*-pyrazol-3-yl]-*N*-methylaniline (**5**).



To a solution of isomeric mixture *tert*-butyl {4-[3-(3-bromophenyl)-1-methyl-1*H*-pyrazol-5-yl]phenyl}methylcarbamate (**14a**) and *tert*-butyl {4-[5-(3-bromophenyl)-1-methyl-1*H*-pyrazol-3-yl]phenyl}methylcarbamate (**14b**) (403 mg, 910 μ mol) in CH_2Cl_2 (5 mL) trifluoroacetic acid (1 mL, 1.48 g, 13 mmol) was added and the mixture was stirred at RT for 4 h. TLC analysis (SiO_2 , hexane:EtOAc = 3:1, educt R_f = 0.31-0.28, product R_f = 0.26; 0.17) of the quenched small portion of the mixture showed absence of the starting material. Isomers ratio was determined by HPLC and LC-MS chromatography on RP C18 column with gradient water (+0.1% TFA): acetonitrile (+0.1% TFA) 0 \rightarrow 100% in 30 min. The ratio of peak 1 (RT 21.3 min): peak 2 (RT 25.0 min) = 68:32 was found. The mixture was concentrated in vacuo, 1 M sodium phosphate buffer pH 7 (20 mL) was added, and the product was extracted with EtOAc (20 mL). The combined extracts were washed with brine, dried over Na_2SO_4 and concentrated in vacuo. The residue was purified on 60 g silica gel (hexane:EtOAc = 3:1, R_f = 0.26; 0.17) to afford **5**, peak 1 (195 mg) and **4**, peak 2 (74 mg). Total yield 269 mg (786 μ mol, 86%). Attempt to isolate the products as free base in solid form failed. To the solutions of products in CH_2Cl_2 (10 mL) 5 M HCl/*i*PrOH solution (400 μ L for each) was added, evaporated, and dried *in vacuo* afforded hydrochlorides of **5**, peak 1 (226 mg) and **4**, peak 2 (82 mg) as white solids.

4-[3-(3-Bromophenyl)-1-methyl-1*H*-pyrazol-5-yl]-*N*-methylaniline•HCl (**4**, peak 2) ¹H NMR (400 MHz, DMSO-*d*₆): δ = 8.00 (t, *J* = 1.5 Hz, 1 H), 7.83 (d, *J* = 7.7, 1 H), 7.69 (d, *J* = 8.5 Hz, 2 H), 7.57 (d, *J* = 8.4, 2 H), 7.49 (d, *J* = 8.3 Hz, 1 H), 7.38 (t, *J* = 7.9 Hz, 1 H), 7.00 (s, 1 H), 3.91 (s, 3 H), 2.91 (s, 3 H). ¹³C-NMR (75 MHz, DMSO-*d*₆): δ = 147.7, 144.0, 140.1, 135.6, 131.1, 130.4, 130.0, 128.3, 127.6, 124.1, 122.4, 121.5, 104.0, 38.1, 35.0. ESI-MS: *m/z* (MeCN, positive mode): calcd for C₁₇H₁₇⁷⁹BrN₃ [M+H]⁺: 342.06 found: 342.52. m.p.: 181 °C.

4-[5-(3-bromophenyl)-1-methyl-1*H*-pyrazol-3-yl]-*N*-methylaniline•HCl (**5**, peak 1) ¹H NMR (400 MHz, DMSO-*d*₆): δ = 7.95 (d, *J* = 8.5, 2 H), 7.81 (t, *J* = 1.7 Hz, 1 H), 7.67 (dd, *J* = 7.8, 1.6 Hz, 1 H), 7.62 (d, *J* = 7.9, 1 H), 7.59 (d, *J* = 8.6 Hz, 2 H), 7.49 (t, *J* = 7.8 Hz, 1 H), 7.04 (s, 1 H), 3.92 (s, 3 H), 2.91 (s, 3 H). ¹³C-NMR (75 MHz, DMSO-*d*₆): δ = 148.1, 143.3, 137.5, 133.3, 132.3, 131.7, 131.2 (2C), 127.7, 126.4, 122.8, 122.3, 104.3, 38.1, 35.9. ESI-MS: *m/z* (MeCN, positive mode): calcd for C₁₇H₁₇⁷⁹BrN₃ [M+H]⁺: 342.06 found: 342.46. m.p.: 202 °C.

Non-radioactive methylation reactions

Methylations were performed by direct methylation with methyl iodide (Method A) or reductive methylation (Method B) as illustrated in Supplemental Scheme 6.

Method A

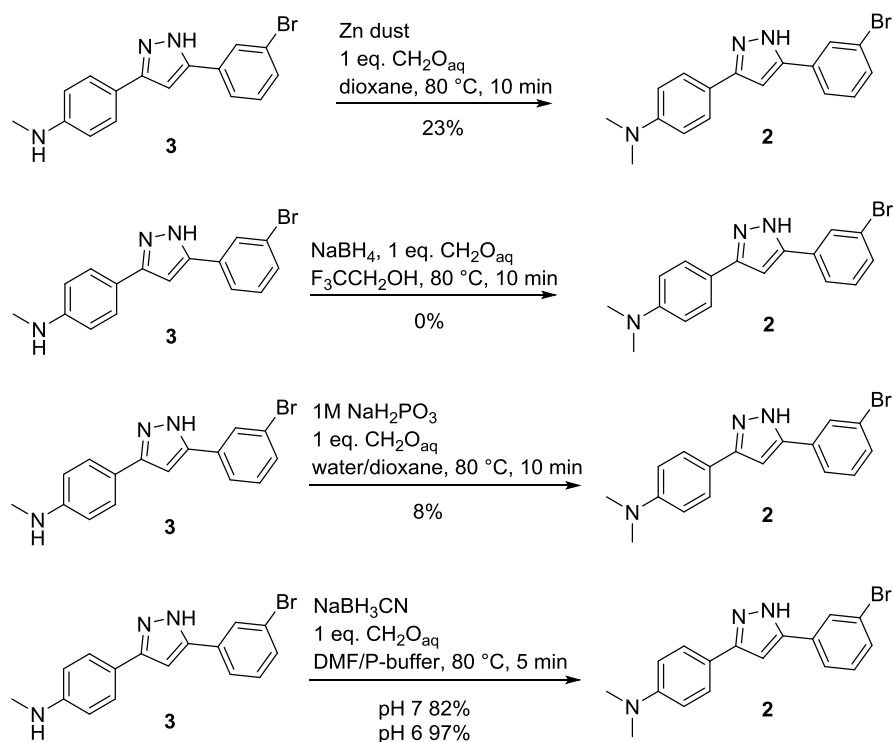
A mixture of **3** (5-10 mg), base (if required) and MeI in DMSO (110-2500 μL) in a reaction vessel with a screw cap was heated under stirring for 15-30 min. After cooling to RT in the water bath an aliquot (50 μL) of the mixture was sampled, diluted with CH₃CN (950 μL) and analyzed by HPLC. The experimental conditions, including reagent ratio, reaction time and temperature, are summarized in Supplemental Table 1.

Method B

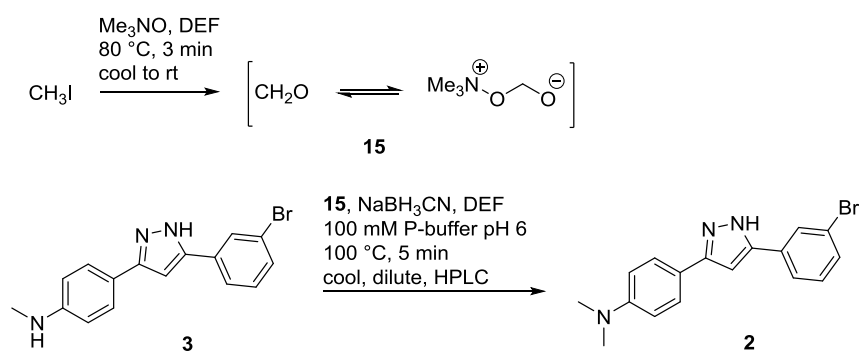
A 5 mL reaction vessel with screw cap was charged with a magnetic stirring bar, trimethylamine *N*-oxide (5 mg, 66.6 μmol), and *N,N*-diethylformamide (DEF) (300 μL). A freshly prepared solution of MeI 1): (0.43 mg, 3.05 μmol); 2): (0.043 mg, 0.0305 μmol); 3): (0.0043 mg, 0.00305 μmol)] in DEF (10 μL) was added. The sealed vessel was heated with stirring in preheated oil bath at 80 °C for 3 min and then cooled to RT in a water bath. The vessel was opened, a solution of **3** (1 mg, 3.05 μmol) in DEF (50 μL), 1 M solution of NaBH₃CN in DEF (60 μL, 60 μmol), and 100 mM citric acid-Na₂HPO₄ buffer solution pH 5 (for preparation see SigmaAldrich Buffer Reference Center) (1 mL) were added subsequently, the vessel was sealed and heated with stirring in preheated oil bath at 100 °C for 5 min. After cooling to RT in a water bath an aliquot (100 μL) of the mixture was sampled, diluted with 50% v/v aqueous CH₃CN (900 μL) and analyzed by HPLC. A composition of reaction mixtures is summarized in Supplemental Table 1.

Synthesis of quinuclidine-*N*-oxide (QNO)

Quinuclidine was oxidized as previously described.^[8] Briefly, 4.5 mmol quinuclidine (0.5 g) were diluted with 5 mL ethanol and chilled on ice. After dropwise addition of 3 mL 30% H₂O₂ the solution was slowly warmed to RT and stirred for three days. Absence of non-oxidized quinuclidine was verified using pH test strips and the bulk solvents were removed under reduced pressure. Vacuum-drying (10⁻³ mbar) of the remaining oil for several days quantitatively yielded highly hygroscopic crystals of quinuclidine-*N*-oxide. ESI-MS: 128.2 [M+H]⁺ (calculated: 128.107). ¹H NMR (600 MHz, D₂O): δ 3.31-3.25 (m, 6H), 1.97-1.91 (m, 7H). ¹³C NMR (150 MHz, D₂O): δ 62.04, 25.62, 19.20.



Supplemental Scheme 3: Screening for suitable reduction conditions for reductive methylation yielding **2**.



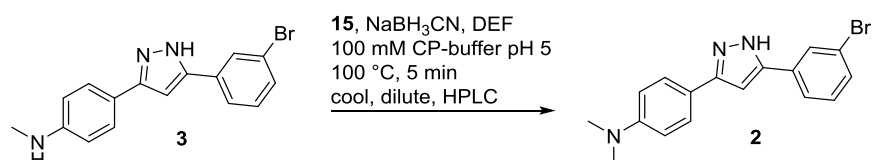
CH₃I:3 = 1:1 yield^[a] **2**: 47%

CH₃I:3 = 1:10 yield^[a] **2**: 28%

CH₃I:3 = 1:100 yield^[a] **2**: 39%

^[a]based on amount of MeI and calculated on peak area of the products and starting materials in HPLC

Supplemental Scheme 4: Correlation of the chemical conversion with methyl iodide excess.



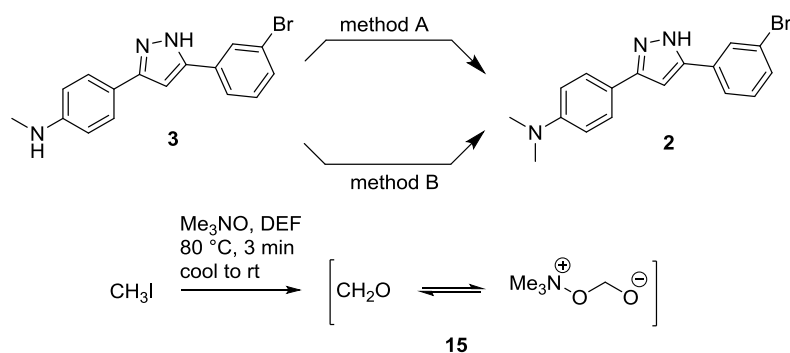
CH₃I:3 = 1:1 yield^[a] **2**: 53%

CH₃I:3 = 1:10 yield^[a] **2**: 26%

CH₃I:3 = 1:100 yield^[a] **2**: 51%

^[a]based on amount of MeI and calculated on peak area of the products and starting materials in HPLC

Supplemental Scheme 5: Correlation of the chemical conversion with methyl iodide excess at pH 5.



Supplemental Scheme 6: Methylation of **3**. Method A: **3**, MeI, base. Method B: **3**, **15**, NaBH₃CN.

Supplemental Table 1: Optimization of non-radioactive methylation of **3**.

Entry	Method	MeI: 3 molar ratio	Time, min	Temp, °C	Base, (equiv) ^a	3 , mg/ml ^b	MeI conversion [%] ^c	
							2	4/5
1	A	1:10	20	80	-	45	67	trace
2	A	1:10	20	80	NaHCO ₃ (10)	45	35	48
3	A	1:10	20	80	Cs ₂ CO ₃ (5)	45	trace	100
4	A	1:100	15	90	-	45	85	trace
5	A	1:100	15	110	-	2	17	trace
6	A	1:100	15	110	-	50	66	trace
7	A	1:1000	30	110	-	2	trace	trace
8	A	1:1000	15	110	-	50	35	trace
9	B	1:1	8	100	-	0.7	53	-
10	B	1:10	8	100	-	0.7	26	-
11	B	1:100	8	100	-	0.7	51	-

^a) based on amount of MeI.

^b) concentration of **3** in the reaction mixture.

^c) calculated based on peak area of the products and starting materials in HPLC.

Production of [¹¹C]methyl iodide and [¹¹C]methyl triflate

[¹¹C]CO₂ was prepared by bombardment of ¹⁴N₂ target gas containing 1 % O₂ with 70 μA of 16.5 MeV protons using a PETtrace 860 cyclotron (GE Healthcare). [¹¹C]methyl iodide and [¹¹C]methyl triflate were produced via gas phase conversion^[9] using a Tracerlab FX MeI module (GE Healthcare) according to the manufacturer's recommendations and transferred to a Tracerlab FX M module (GE Healthcare).

Substitutive radiomethylation of **3**

The alkylating reagent was bubbled through a cooled solution (-25 °C for DMF, 18 °C for DMSO) of 1 mg **3** and a helper base in 300 μL organic solvent. After the reaction time at elevated temperature (main manuscript, Table 1) the solution was diluted with 1.2 mL of HPLC eluent and subjected to isocratic semipreparative HPLC on a Synergi 4 μm Max-RP 80 Å column (250×10 mm, Phenomenex) with 6 mL/min of 65% acetonitrile in water.

Reductive radiomethylation of **3**

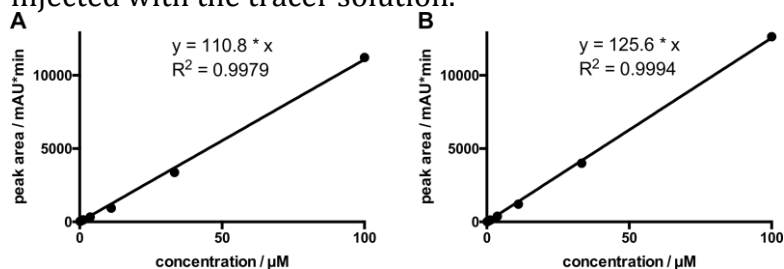
[¹¹C]methyl iodide was trapped in a solution of 5 mg Me₃NO and 1 mg **3** in 350 μL diethyl formamide cooled to -25 °C. After heating to 60 °C for 3 min the reactor was cooled to 40 °C and 7.6 mg NaBH₃CN were added in a mixture of 60 μL diethyl formamide and 1.2 mL 100 mM citrate-phosphate buffer pH 5. After heating to 100 °C for 5 min, the crude reaction was subjected to semipreparative HPLC (Phenomenex Synergi 4 μm Max-RP 80 Å, 250×10mm, 5 mL/min 65% acetonitrile in water).

Formulation of [¹¹C]**2**

The HPLC fraction containing the product was diluted with 50 mL water and loaded onto a Sep-Pak C8 Plus Light cartridge (Waters). After washing the cartridge with 5 mL of water the product was eluted with 500 μL ethanol and diluted with 5 mL of phosphate-buffered saline (Gibco DPBS without calcium and magnesium, Thermo Fisher). Activity was measured using a VDC-405 dose calibrator (Comer) and samples were drawn for analysis before the remaining product was used for *in vitro* and *in vivo* experiments.

[¹¹C]**2** quality control and calculation of specific activity

100 μL of the tracer solution were injected onto a Luna Phenyl-Hexyl column (5 μm, 100 Å, 300×4.6 mm, Phenomenex) using a 1260 Infinity HPLC system (Agilent Technologies) equipped with autosampler, NaI(Tl) scintillator system and the multi-wavelength detector set to 254 nm. 50 % acetonitrile in 0.1 % aqueous trifluoroacetic acid was used as mobile phase for isocratic separation at a flow of 1.5 mL/min. Carrier content was calculated from linear regression of a calibration curve (Supplemental Figure 4) of both **3** and **2** in the range of 0.1-100 μM. For identity verification non-radioactive **2** was co-injected with the tracer solution.



Supplemental Figure 4: Calibration curves for **3** (left) and **2** (right) HPLC integrals.

Serum stability analysis

Rat blood was obtained by heart punctation using Multivette 600 Z tubes (Sarstedt, Nümbrecht, Germany) and centrifuged at RT for 5 minutes at 1000×g according to the manufacturer's instructions. The serum was aliquoted and snap-frozen in liquid nitrogen. The tracer formulation was mixed with an equal volume of rat serum and incubated at 37 °C. At different time points samples were analyzed by radio-HPLC. Each sample was immediately mixed with 1 volume of acetonitrile and incubated for 3 minutes on ice before precipitated proteins were removed by centrifugation for 5 min at 12100×g using a MiniSpin centrifuge (Eppendorf). 100 μL of the supernatant were subjected to analytical HPLC as described in the previous paragraph.

Production of αSyn fibrils

Expression and purification of recombinant wildtype αSyn was performed as previously described.^[10] Briefly, pET-5a/α-synuclein (136TAT) plasmid (wt-plasmid by Philipp Kahle, Hertie Institute for Clinical Brain Research, Tübingen; 136-TAC/TAT-Mutation by Matthias Habek, LMU Munich) was used to transform *E. coli* BL21(DE3)pLys (Novagen,

Madison, WI, USA), and expression was induced with isopropyl- β -D-thiogalactopyranose (IPTG, Peqlab, Erlangen, Germany). Cells were lysed by boiling after heat-inactivation of proteases. After centrifugation the supernatant was filtered through a Filtropur S 0.2 μ m filter (Sarstedt, Nümbrecht, Germany), loaded on a HiTrap Q HP anion-exchange column (5 mL, GE Healthcare, Munich, Germany) and eluted with a linear gradient of 25 mM to 500 mM NaCl. Fractions containing α Syn were pooled and polished by gel filtration via a Superdex 75 prep grade column (25 mL, GE Healthcare, Munich, Germany). Protein concentration was adjusted to 1 mg/ml in 50mM Tris-HCl, pH 7.0. After freezing in liquid nitrogen the protein was stored at -80°C.

Fibrillization was induced by constant agitation at high protein concentrations.^[11] Briefly, 1 mg/ml α Syn in 50 mM Tris-HCl, containing 100 mM NaCl, 0.02 % NaN₃, pH 7.0 was incubated for 96 h at 37 °C and 1400 rpm using an Eppendorf Thermomixer Comfort (Eppendorf, Hamburg, Germany). To purify the fibrils from un-aggregated monomeric α Syn the fibril preparations were ultracentrifuged with 135,000 \times g at 4 °C for 30 min in a Beckman Optima Max-XP centrifuge (Beckman Coulter, Krefeld, Germany). The pellet was resuspended in the aggregation buffer and the concentration was determined using BCA assay. After freezing in liquid nitrogen fibrils were stored at -80°C.

Fibril characterization

Fibril formation was verified using Thioflavin (Th)T-fluorescence and sucrose density centrifugation. ThT-fluorescence was measured using a LS55 Luminescence Spectrometer (Perkin Elmer, Hamburg, Germany) with molar ratios of 0.5 μ M protein and 20 μ M ThT (Sigma Aldrich, Taufkirchen, Germany) in 50 mM Tris-HCl, pH 7. Spectra were recorded for wavelengths ranging from 460 to 560 nm.

Continuous sucrose-gradient assay was performed as described previously.^[3, 12] Briefly, solutions containing 50 mM Tris, pH 7.5 containing 0.1% NP-40 (Roche, Mannheim, Germany) and sucrose (10%, 20%, 30%, 40%, 50% and 60%, respectively; Hartenstein, Würzburg, Germany) were filled into a 4 mL 11 \times 60 mm polyallomer tube (Beckman coulter, Krefeld, Germany) beginning with 200 μ L of 60% sucrose solution loaded to the bottom, then followed by 400 μ L of 50% to 10% sucrose. Finally, 200 μ L of 5 μ M protein in 1 \times TBS (pH 7.5) containing 0.1% NP-40 were loaded on the top of the gradient. Ultracentrifugation with 100,000 \times g at 4 °C for 1 h was performed in a Sorvall WX Ultra 90 centrifuge using a Sw60Ti rotor (Beckman Coulter, Krefeld, Germany). Resulting continuous gradients were fractionated in volumes of 200 μ L. 20 μ L per fraction were analyzed by denaturing SDS-PAGE and Western blot using 4B12, a monoclonal antibody against human α Syn (Hiss, Freiburg, Germany).

α Syn fibril binding assay for ¹¹C

All experiments were performed in triplicate wells for each condition. Fibrils (100 pmol/well in 100 μ L PBS) were immobilized on F-bottom high binding ELISA plates (Greiner Bio-One, Frickenhausen, Germany) over night at 4 °C. After one hour of blocking with 1 % BSA at RT and three subsequent washing steps with PBS-T, the fibrils were probed with 3 nM [¹¹C]**2** in incubation buffer (50 mM Tris pH 7.4, 10 % ethanol, 0.05 % Tween 20) for 30 minutes at RT in the presence or absence of a blocking concentration (1 μ M) of non-radioactive **2** (DMSO concentration of 0.1 % in all samples). After removal of the unbound tracer and three washing steps with the incubation buffer the plates were analyzed by autoradiography (12 half-lives exposition) using a Storm 840 phosphorimager (GE Healthcare) and phosphor screens. Autoradiographs were analyzed in ImageJ 1.46r. Images were converted to 32 bit and pixel values were

squared before regions of interest (ROI) were defined and quantified. Non-exposed areas of the images were used as background regions and subtracted from the median ROI values. Median and standard deviation were plotted and one-way ANOVA followed by Dunnett's or Tukey's (depending on the experimental design) multiple comparisons test was performed using GraphPad Prism version 6 (GraphPad Software, La Jolla).

Tritium binding assay

Anle138b (**1**) was synthesized as described before,^[3] and catalytically tritiated by a commercial service provider (RC Tritec AG, Teufen, Switzerland). For the competition binding assay, 50 μL of a mixture of αSYN monomers, oligomers and fibrils (31 nM final concentration diluted in PBS) was added to a 96 well low binding plate (96-well micro test plate, ratiolab GmbH, Dreieich, Germany). 1:4 serial dilutions of **2** starting from 62.5 nM final concentration were prepared in assay buffer (50 mM Tris, 10 % EtOH, 0.05 % Tween20, pH 7.4). [³H]**1** (1 nM final concentration diluted in assay buffer) was first mixed with the dilutions of **2** and then pipetted onto the fibrils (150 μL). A plastic foil (Resealable tape, PerkinElmer, Waltham, MA, USA) was used to cover the plates to avoid evaporation during a 2 hours incubation time with constant agitation at a temperature of 37 °C. After incubation, bound and free ligands were separated by vacuum filtration using a harvester (Filtermate harvester, PerkinElmer, Waltham, MA, USA). The filter (Printed filtermat B, PerkinElmer, Waltham, MA, USA) was washed twice with around 50 mL assay buffer cooled to 4 °C, subsequently dried in the microwave for 2 minutes at medium power and sealed in a plastic bag together with approximately 12 mL added liquid scintillator. Tritium was quantified in a liquid scintillation counter (Wallac MicroBeta® TriLux, 1450 LSC & Luminescence Counter, PerkinElmer, Waltham, MA, USA). After subtraction of the background values, radioactivity was plotted against the increasing competitor concentrations. Data points were fitted in GraphPad Prism (GraphPad Software, Inc., Version 7.03, La Jolla, CA, USA) using non-linear regression analysis.

Dynamic biodistribution analysis

PET measurements were performed on two dedicated small animal Inveon PET scanners (Siemens Healthcare, Knoxville, TN, USA). Four twelve-week-old healthy female Sprague Dawley rats were kept under 1.5 % isoflurane anesthesia evaporated in 100 % oxygen (0.8 L/min). During each scan, two rats were positioned head-to-head in the center of the field of view on a carbon fiber bed (Siemens Healthcare) on the PET scanner. The temperature of the animals was monitored using a rectal probe and maintained at about 37°C using a feedback control unit and heating mat (Föhr Medical Instruments, Seeheim-Ober-Beerbach, Germany). Each rat was injected intravenously with 27.1 ± 0.2 MBq of [¹¹C]**2** using a tail vein catheter which was flushed with 100 μL of saline to inject the remaining activity. The acquisition started five seconds prior to the bolus injection of the tracer and 60 minutes dynamic PET measurements were acquired for all rats with a 13-minute ⁵⁷Co transmission scan at the end. The list-mode data from the dynamic acquisitions were histogrammed into 39 time frames (12×5, 6×10, 6×30, 5×60, and 10×300 s). Images were reconstructed using filtered backprojection and a matrix size of 256×256×159, resulting in a pixel size of 0.39×0.39×0.80 mm³.

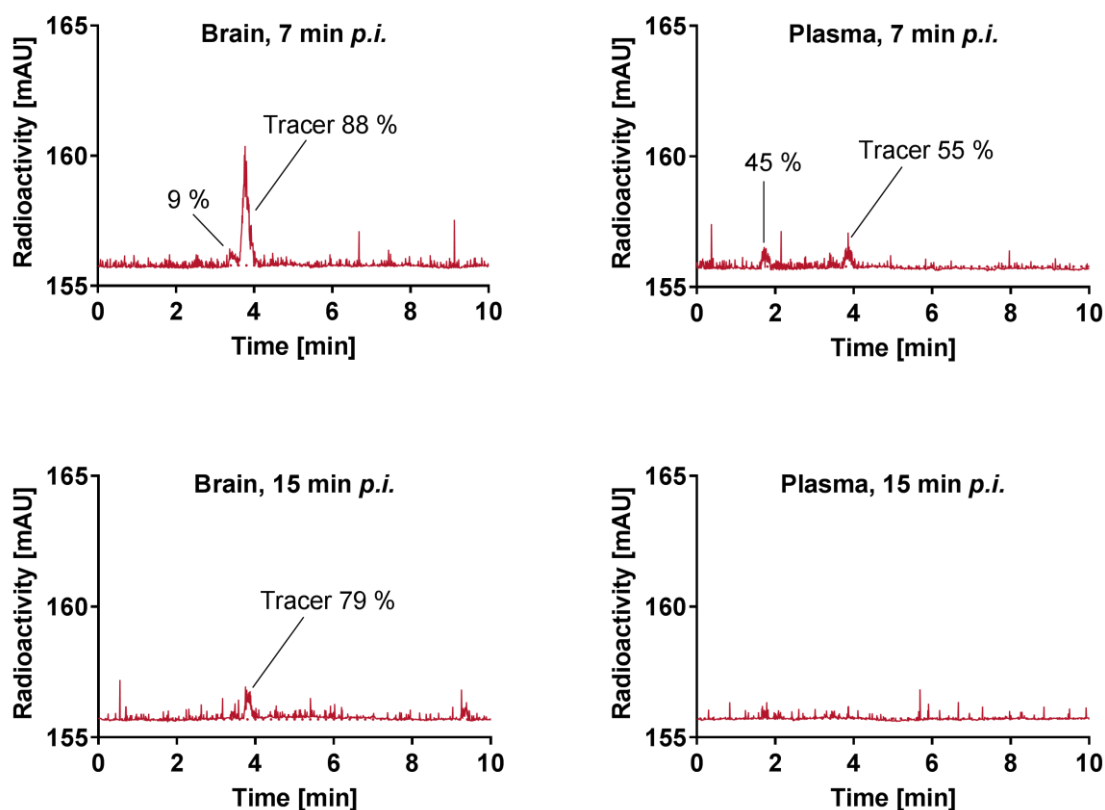
The analysis of the data, including alignment of PET images to the Schiffer atlas ^[13] for volumes of interest (VOIs) definition was performed using PMOD software (version 3.2; PMOD Technologies, Zürich, Switzerland). The results are shown as %ID/cm³ and are presented as mean \pm standard deviation.

After the PET acquisition, retrobulbar blood samples were taken from all animals. Subsequently, the animals were dissected for biodistribution analysis. The brain (cortex, striatum, brainstem, cerebellum), heart, left and right kidney, liver, lung and muscle were removed and measured using gamma counting. The concentration of the activity in all samples was measured with a WIZARD2 gamma counter (Perkin Elmer). The results are expressed as percentage of injected dose per gram (%ID/g) of the tissue.

In vivo stability analysis

Two female Sprague Dawley rats (10 w, 259 ± 16 g) were anaesthetized with 1.75 % isoflurane evaporated in 100 % oxygen at a flow rate of 0.8 L/min. Anesthesia and heating were maintained during the entire experiment. Each rat was i.v. injected with 178 ± 36 MBq of [^{11}C]2 using a tail vein catheter, which was flushed with 50 μL of saline to inject the remaining activity. A blood sample was collected by heart puncture 7 and 15 minutes post tracer injection. The blood was centrifuged at $17.000 \times g$ and 4°C for 2 minutes and the plasma was transferred to a 1.5 mL reaction tube on ice for further analysis. In parallel, rats were transcordially perfused (50 mL/min) with 100 mL ice-cold PBS and the brain was surgically removed. The right brain hemisphere was transferred to a glass tube (2 mL dounce tissue grinder set, Sigma Aldrich Chemie GmbH, Taufkirchen, Germany) containing 0.5 mL ice-cold PBS, homogenized using large and small clearance pestles sequentially and transferred to a 1.5 mL reaction tube on ice for further analysis. Plasma and brain homogenate were diluted 1:1 with acetonitrile, mixed in a vortex mixer followed by another centrifugation step for 1.5 min at $12,100 \times g$ in a MiniSpin centrifuge (Eppendorf, Hamburg, Germany) to remove precipitated proteins. The supernatants were analyzed by radio-HPLC as described in the quality control section.

For data analysis, the median of five consecutive data points was calculated to remove noise. In GraphPad Prism, radioactivity was plotted against time and data were analyzed by integration analysis (Area Under Curve (AUC) function in GraphPad) to get information about the peak area, peak height and the retention time (tR) of considerable peaks.



Supplemental Figure 5: Radio-HPLC analysis of brain lysate and plasma after injection of [^{11}C]2. The tracer 2 constituted the main radioactivity peak in the brain both at 7 and 15 min post injection. Peak areas (%) are shown although the low sensitivity of the setup does not allow precise detection of minor peaks.

Supplemental References

- [1] W. L. F. Armarego, C. L. L. Chai, *Purification of Laboratory Chemicals, 6th Edition* **2009**, 1-743.
- [2] R. Lindner, University of Goettingen **2013**.
- [3] J. Wagner, S. Ryazanov, A. Leonov, J. Levin, S. Shi, F. Schmidt, C. Prix, F. Pan-Montojo, U. Bertsch, G. Mitteregger-Kretschmar, M. Geissen, M. Eiden, F. Leidel, T. Hirschberger, A. A. Deeg, J. J. Krauth, W. Zinth, P. Tavan, J. Pilger, M. Zweckstetter, T. Frank, M. Bahr, J. H. Weishaupt, M. Uhr, H. Urlaub, U. Teichmann, M. Samwer, K. Botzel, M. Groschup, H. Kretschmar, C. Griesinger, A. Giese, *Acta Neuropathol* **2013**, *125*, 795-813.
- [4] Y. Lin, S. A. Lang, *J Heterocyclic Chem* **1980**, *17*, 1273-1275.
- [5] K. P. Dhake, P. J. Tambade, R. S. Singhal, B. M. Bhanage, *Green Chem Lett Rev* **2011**, *4*, 151-157.
- [6] H. C. Brown, Y. M. Choi, S. Narasimhan, *J Org Chem* **1982**, *47*, 3153-3163.
- [7] T. Tago, S. Furumoto, N. Okamura, R. Harada, Y. Ishikawa, H. Arai, K. Yanai, R. Iwata, Y. Kudo, *J Labelled Comp Radiopharm* **2014**, *57*, 18-24.
- [8] S. Srinivas, K. G. Taylor, *J Org Chem* **1990**, *55*, 1779-1786.
- [9] P. Larsen, J. Ulin, K. Dahlstrom, M. Jensen, *Appl Radiat Isotopes* **1997**, *48*, 153-157.
- [10] B. Nuscher, F. Kamp, T. Mehnert, S. Odoy, C. Haass, P. J. Kahle, K. Beyer, *J Biol Chem* **2004**, *279*, 21966-21975.
- [11] aK. A. Conway, J. D. Harper, P. T. Lansbury, *Biochemistry-Us* **2000**, *39*, 2552-2563;
 bA. A. Deeg, A. M. Reiner, F. Schmidt, F. Schueder, S. Ryazanov, V. C. Ruf, K. Giller,

- S. Becker, A. Leonov, C. Griesinger, A. Giese, W. Zinth, *Bba-Gen Subjects* **2015**, *1850*, 1884-1890; cA. L. Fink, in *Misbehaving Proteins: Protein (Mis)Folding, Aggregation, and Stability*, Springer New York, New York, NY, **2006**, pp. 265-285.
- [12] S. Tzaban, G. Friedlander, O. Schonberger, L. Horonchik, Y. Yedidia, G. Shaked, R. Gabizon, A. Taraboulos, *Biochemistry-Us* **2002**, *41*, 12868-12875.
- [13] W. K. Schiffer, M. M. Mirrione, A. Biegon, D. L. Alexoff, V. Patel, S. L. Dewey, *J Neurosci Methods* **2006**, *155*, 272-284.